

# Tough, high-strength, flame-retardant and recyclable polyurethane elastomers based on dynamic borate acid esters

Tiantian Zhang<sup>a</sup>, Siqi Huo<sup>b,\*</sup>, Guofeng Ye<sup>a</sup>, Cheng Wang<sup>a</sup>, Qi Zhang<sup>a</sup>, Zhitian Liu<sup>a,\*</sup>

<sup>a</sup> Hubei Engineering Technology Research Center of Optoelectronic and New Energy Materials, School of Materials Science & Engineering, Wuhan Institute of Technology, Wuhan 430205, China

<sup>b</sup> Centre for Future Materials, School of Engineering, University of Southern Queensland, Springfield 4300, Australia

## ARTICLE INFO

### Keywords:

Polyurethane elastomer  
Transparency  
Flame retardancy  
Mechanical properties  
Recyclability

## ABSTRACT

With the wide application of polyurethane elastomers, it is necessary to develop recyclable, fire-retardant polyurethane elastomers with great mechanical properties to comply with industrial requirements. Herein, we fabricated a flame-retardant, recyclable, strong yet tough polyurethane elastomer (PIDB-1) based on dynamic borate acid esters. The introduction of phosphaphenanthrene and boron-containing groups endow PIDB-1 with great flame retardancy, as reflected by it achieving the vertical burning (UL-94) V-0 rating. The PIDB-1 film shows high visible light transmittance, and its transmittance reaches 90 % at the wavelength of 800 to 900 nm. The tensile strength of PIDB-1 is 54.9 MPa, and its toughness reaches 207.8 kJ/m<sup>3</sup>, indicative of superior mechanical properties. Meanwhile, the dynamic borate acid esters allow the PIDB-1 elastomer to possess physical and chemical recyclability. When using PIDB-1 as a polymer matrix for carbon fiber-reinforced polymer composites, the carbon fibers can be fully recycled. This work provides an integrated design strategy for creating transparent, flame-retardant, recyclable polyurethane elastomers combining high strength and toughness based on dynamic borate ester bonds, which is expected to find wide applications in different industries.

## 1. Introduction

Polyurethane elastomers find extensive application across various sectors such as automotive [1,2], electronics [3–5], medical devices [6,7], and sports equipment [8,9] due to their remarkable elasticity and wear resistance. They are categorized into thermosetting and thermoplastic types. Thermoplastic polyurethane elastomers can be melted and reprocessed, offering good processability and recyclability [10]. However, thermosetting polyurethane elastomers will form a three-dimensional cross-linking network during curing, thus they are unable to reprocess. Traditionally, discarded thermosetting polyurethane elastomers are disposed of by crushing, incineration, and landfill, bringing about resource waste and environmental risks. Hence, there is a critical need to develop strong, tough and recyclable thermosetting polyurethane elastomers [11–13].

In recent years, much attention has been focused on the creation of recyclable thermosetting polymers through introducing dynamic covalent bonds. Dynamic covalent bonds can exchange rapidly under certain conditions, resulting in the rearrangement of topological structure for thermosetting polymers. The first recyclable thermosetting polymer,

named vitrimer, was synthesized by Leibler and co-workers in 2011, which opened an innovative era in the field of polymeric materials [14]. Then, various dynamic covalent bonds have been reported and applied in recyclable polymers, including disulfide bond [15–19], imine bond [17,20,21],  $\beta$ -hydroxyl ester bond [22,23], and borate ester bond [24–27].

Chen [28] et al. reported a high-performance waterborne polyurethane vitrimer with reprocessability by introducing dynamic aromatic disulfide bonds into the polyurethane polymer chain network. The obtained vitrimer achieved a tensile strength of 30.95 MPa, and its mechanical performances were well maintained after three reprocessing cycles. Liu et al. [29] synthesized a bio-based imine-containing polyurethane vitrimer, and its tensile strength and elongation at break reached 38.7 MPa and 347.6 %, respectively. Moreover, it could be recycled and healed at 80 °C. All these works confirm that introducing dynamic covalent bonds into polyurethane elastomer can impart recyclability and reprocessability to it. However, the development of tough and strong polyurethane elastomer vitrimer is still challenging yet necessary.

Polyurethane, as a common polymeric material, is highly flammable,

\* Corresponding authors.

E-mail addresses: [Siqi.Huo@unisuq.edu.au](mailto:Siqi.Huo@unisuq.edu.au), [sqhuo@hotmail.com](mailto:sqhuo@hotmail.com) (S. Huo), [able.ztliu@wit.edu.cn](mailto:able.ztliu@wit.edu.cn) (Z. Liu).

<https://doi.org/10.1016/j.reactfunctpolym.2024.106056>

Received 31 May 2024; Received in revised form 13 September 2024; Accepted 14 September 2024

Available online 16 September 2024

1381-5148/© 2024 The Authors. Published by Elsevier B.V. This is an open access article under the CC BY license (<http://creativecommons.org/licenses/by/4.0/>).

which seriously affects its application. Although adding flame retardants is a common way to enhance flame retardancy, they usually suffer from poor compatibility with the polyurethane matrix, thus seriously reducing mechanical properties [30]. To solve the above problems, we developed a flame-retardant, tough, strong and recyclable polyurethane elastomer (PIDB-1) with dynamic borate ester bonds using isophone diisocyanate, poly(tetrahydrofuran), DOPO-containing amine, and boric acid. PIDB-1 passes an UL-94 V-0 rating, indicative of great flame retardancy. Additionally, PIDB-1 shows a tensile strength of 54.9 MPa and an elongation at break of 891 %, demonstrating superior mechanical properties. Due to the dynamic borate ester bonds, PIDB-1 features physical and chemical recyclability, and thus it can be used as a polymer matrix for recyclable carbon fiber-reinforced polymer composites. Therefore, this work provides a rational method for the creation of polyurethane elastomer vitrimers with superior mechanical properties, flame retardancy and recyclability based on dynamic borate esters.

## 2. Experiment section

### 2.1. Materials

Anhydrous methanol was purchased from Sinopharm Chemical Reagent Co., Ltd. (Shanghai, China). *p*-Toluenesulfonic acid (*p*-TSA) was provided by McLean Biochemical Technology Co., Ltd. (Shanghai, China). 9,10-Dihydro-9-oxa-10-phosphaphenanthrene-10-oxide (DOPO) was obtained from Aladdin Chemistry Co., Ltd. (Shanghai, China). Dibutyltin dilaurate (DBTDL, 98 %), *N,N*-dimethylacetamide (DMAc, 99.8 %), poly(tetrahydrofuran) (PTMEG, number average molecular weight ( $M_n$ ) of ~2000), isophone diisocyanate (IPDI), 4'-aminoacetophenone, and aniline were provided by Sarn Chemical Technology Co., Ltd. (Shanghai, China). The DOPO-containing amine was synthesized based on a previous work [31], and its synthesis route and  $^1\text{H}$  and  $^{31}\text{P}$  nuclear magnetic resonance (NMR) are shown in Fig. S1-S3. Unidirectional carbon fiber fabric (areal density: 200 g/m<sup>2</sup>) was purchased from Zhongfu Shenying Carbon Fiber Co., Ltd. (Jiangsu, China). All chemicals were used directly without further purification.

### 2.2. Synthesis of PIDB elastomers

Firstly, the glass instruments were pre-dried at 100 °C, and PTMEG underwent a 2-h drying in a vacuum oven at 100 °C. Then, PTMEG (10 g, 5 mmol) and IPDI (4.45 g, 20 mmol) were added into a three-necked glass flask, followed by the addition of 1 to 2 drops of DBTDL. The mixture was stirred for 2.5 h at 80 °C under nitrogen atmosphere. After

cooling to 60 °C, DOPO-NH<sub>2</sub> (2.67 g, 6.25 mmol) dissolved in 20 mL of the dry DMAc was added to the flask, and the mixture was stirred for 3.5 h. Boric acid (0.36 g, 5.83 mmol) was dissolved in 10 mL of the dry DMAc and then added into the mixture. The mixture was stirred for 15 min and then poured into a mold. Finally, a colorless and transparent PIDB film sample was obtained after curing at 80 °C for 10 h. PID is a control sample without boric acid, and its preparation process is in line with that of PIDB. The synthesis of PIDB is illustrated in Fig. 1, and its formulation is shown in Table 1.

### 2.3. Characterization

The light transmittance of the film (wavelength range: 200–900 nm) was investigated by using ultraviolet-visible (UV-vis) spectroscopy (Lambda35, PerkinElmer, USA) and the film thickness was  $0.20 \pm 0.02$  mm. Fourier transform infrared spectroscopy (FTIR) was conducted on a Nicolet 6700 spectrometer (Thermo Fisher, USA) by KBr compression method with wavenumber range of 4000 to 400 cm<sup>-1</sup>. The chemical structure of DOPO-NH<sub>2</sub> was characterized by  $^1\text{H}$  and  $^{31}\text{P}$  nuclear magnetic resonance spectroscopy (NMR, DD2 400-MR, Agilent, USA), and DMSO-*d*<sub>6</sub> was used as a solvent. X-ray photoelectron spectroscopy (XPS) was performed on a Leybold X-ray photoelectron spectrometer (Thermo Fisher Company, USA) with Al K $\alpha$  radiation (1486.6 eV).

The tensile properties were studied on a 5966 universal testing machine (INSTRON, USA) at a speed of 50 mm/min, and the dumbbell-shaped splines with a size of 0.5 mm × 4.0 mm × 50 mm were used. Five specimens of each formula were tested, and the average values were reported.

According to ASTM D3163, the single lap shear tests of PIDB-1 on different substrates were carried out on a 5966 universal testing machine (INSTRON, USA) at a speed of 5 mm/min. Five specimens of each formula were tested, and the average values were reported.

Dynamic mechanical analysis (DMA) was carried out on a DMA Q800 equipment (TA Instruments, USA) from -100 to 80 °C at a frequency of 1 Hz with a heating rate of 3 °C/min under nitrogen atmosphere. Stress relaxation test was also undertaken on a DMA Q800 equipment. Rectangular specimen with a size of 30.0 mm × 6.0 mm × 1.0 mm was initially aligned by preloading a 0.001 N force, and then thermally equilibrated at each testing temperature for 10 min. The specimen was stretched by 1.0 %, and the strain was retained during the test. The variation in the relaxation modulus as a function of time was recorded.

The cyclic tensile tests of PIDB-1 (specimen size: 0.5 mm × 4.0 mm × 50 mm) were conducted on a 5966 universal testing machine

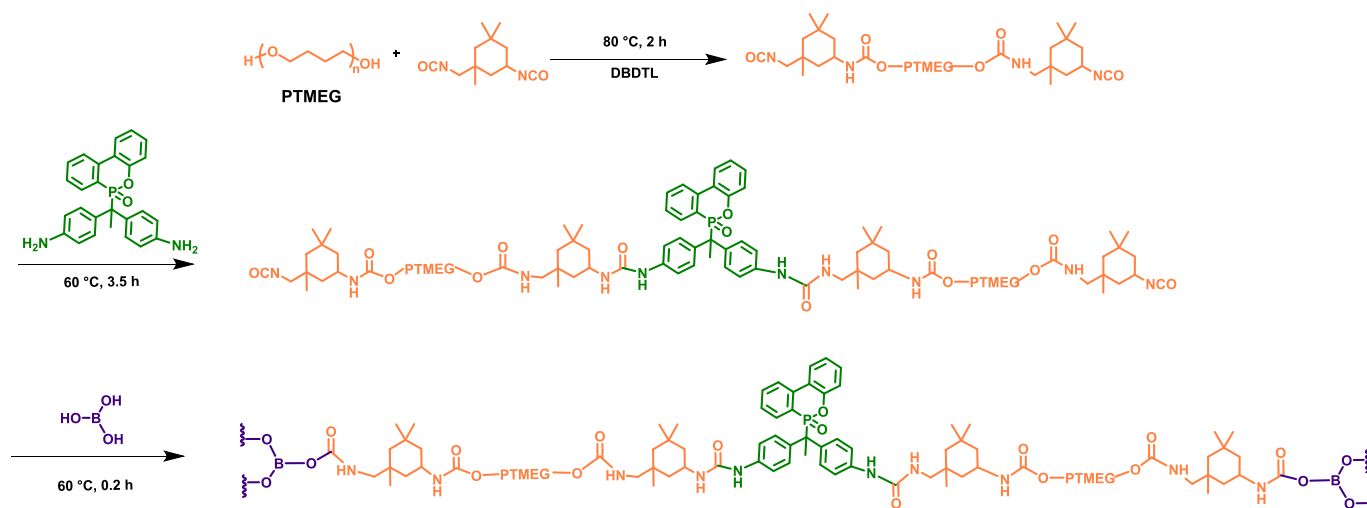


Fig. 1. Synthesis of PIDB.

**Table 1**

The formulations of PIDB and PID elastomers.

| Sample | PTMEG (mmol) | IPDI (mmol) | DOPO-NH <sub>2</sub> (mmol) | Boric acid (mmol) | PTMEG (wt%) | IPDI (wt%) | DOPO-NH <sub>2</sub> (wt%) | Boric acid (wt%) |
|--------|--------------|-------------|-----------------------------|-------------------|-------------|------------|----------------------------|------------------|
| PID    | 5            | 15          | 10                          | 0                 | 64.67       | 21.56      | 13.77                      | 0                |
| PIDB-1 | 5            | 20          | 6.25                        | 5.83              | 57.20       | 25.46      | 15.27                      | 2.07             |
| PIDB-2 | 5            | 25          | 10.0                        | 6.67              | 49.43       | 27.48      | 21.05                      | 2.04             |
| PIDB-3 | 5            | 30          | 15.0                        | 6.67              | 42.60       | 28.44      | 27.20                      | 1.76             |

(INSTRON, USA) at a strain rate of 50 mm/min. The experiment involves a cyclic stretching program with different strain levels ranging from 50 % to 500 %.

The thermogravimetric analysis was carried out on a STA449F3 thermal analyzer (NETZSCH, Germany) from room temperature to 800 °C in nitrogen condition with a heating rate of 10 °C/min. The powdered sample with a mass of approximately 8.0 mg was applied. Microcalorimeter (FTT, UK) was applied to investigate the flame retardancy of sample, and the sample was powder with a mass of 5.0 mg. The vertical burning (UL-94) test was conducted on a CFZ-3 facility (Jiangning Analytical Instrument Co., Ltd., China) according to ASTM D3801 with a specimen size of 120 mm × 13.0 mm × 3.0 mm.

Scanning electron microscopy (SEM) was conducted on a JSW-5510LV microscope (EOL, Japan). Raman spectroscopy was performed by using a DXR laser Raman spectrometer (Thermo Fisher, USA) under 532 nm laser excitation with a wavenumber range of 800 to 2000 cm<sup>-1</sup>.

### 3. Results and discussion

#### 3.1. Transparency and characterization

The transparency of PIDB films was investigated by UV-vis testing, with the spectra shown in Fig. 2a. The transmittance of PIDB-1, PIDB-2 and PIDB-3 films reaches 90 % at the wavelength of 800 to 900 nm,

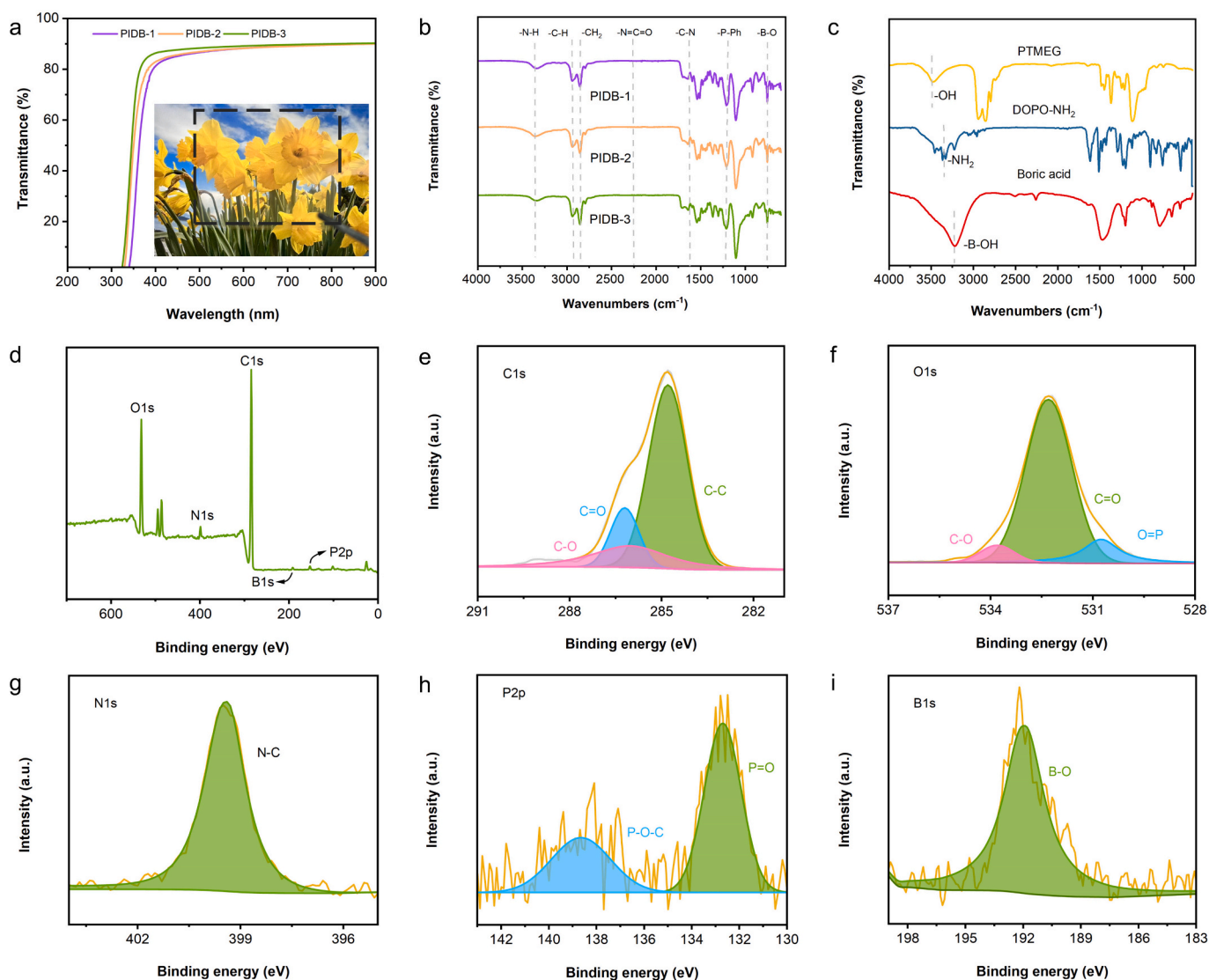


**Fig. 2.** (a) UV-vis transmission spectra of PIDB films and digital photo of PIDB-1, (b) FTIR spectra of PIDB-1, PIDB-2, and PIDB-3, (c) FTIR spectra of PTMEG, DOPO-NH<sub>2</sub>, and boric acid, (d) XPS full-scan spectrum of PIDB-1, and XPS high-resolution (e) C1s, (f) O1s, (g) N1s, (h) P2p, and (i) B1s spectra of PIDB-1.

indicating their high visible-light transmittance. The high transparency of PIDB film can also be confirmed by its digital image in Fig. 2a. Additionally, the increase in DOPO content brings about the reduction in the transmittance of PIDB films below the wavelength of 400 nm, which is mainly due to the UV-shielding effect of the diphenyl group within DOPO [32].

The chemical structures of PIDB elastomers were studied by FTIR and XPS testing. In Fig. 2b, the characteristic peak of  $-N=C=O$  group at  $2250\text{ cm}^{-1}$  cannot be detected in the FTIR spectra of PIDB elastomers [33]. The peaks of  $-OH$  and  $-B-OH$  appear at  $3500$  and  $3200\text{ cm}^{-1}$  in the FTIR spectra of PTMEG and boric acid (see Fig. 2c), but they disappear in the FTIR spectra of PIDB elastomers. These confirm that  $-N=C=O$  of IPDI has reacted with  $-OH$  of PTMEG and  $-B-OH$  of boric acid during the curing process. Moreover, the  $-NH$ ,  $C-N$  and  $P-Ph$  peaks at about  $3322$ ,  $1539$  and  $1740\text{ cm}^{-1}$  in the FTIR spectra of PIDB elastomers indicate that DOPO- $NH_2$  has participated in the curing process. Additionally, the existence of the  $-C-O-B$  and  $-B-O$  peaks at  $1420$  and  $720\text{ cm}^{-1}$  indicates that boric acid has chemically linked to the elastomer network [25,34]. The characteristic peaks of  $-CH_2-$  and  $-CH=$  can be observed at  $2850$  and  $2920\text{ cm}^{-1}$ , respectively, in the FTIR spectra of PIDB elastomers. Thus, these results verify the successful preparation of PIDB elastomers.

The XPS full-scan and high-resolution  $C1s$ ,  $O1s$ ,  $N1s$ ,  $P2p$ , and  $B1s$  spectra of PIDB-1 are presented in Fig. 2d-i. For the  $C1s$  spectrum, it can be deconvoluted into three peaks, belonging to  $C-C/C-H$  ( $284.8\text{ eV}$ ),  $C=O/O-C-O$  ( $286.2\text{ eV}$ ), and  $-C-OH$  ( $285.9\text{ eV}$ ). There are also three deconvoluted peaks in the  $O1s$  spectrum, which are assigned to  $O=P$  ( $530.8\text{ eV}$ ),  $O=C$  ( $532.3\text{ eV}$ ), and  $C-O-B$  ( $533.8\text{ eV}$ ). The  $P2p$  spectrum can be divided into two peaks corresponding to  $P=O$  ( $132.8\text{ eV}$ ) and  $P-O-C$  ( $138.6\text{ eV}$ ). The  $N-C$  ( $399.5\text{ eV}$ ) and  $B-O-C$  ( $191.9\text{ eV}$ ) peaks appear in the  $N1s$  and  $B1s$  spectra, respectively [34–37]. Thus, the XPS results are in line with the FTIR results, further suggesting the successful fabrication of PIDB elastomers.

### 3.2. Mechanical performances of PIDB samples

The glass transition temperature ( $T_g$ ) of polymer material can be characterized by DMA test [29,38]. As shown in the Fig. 3a, the glass transition temperatures of PIDB-1, PIDB-2, and PIDB-3 are  $-61.22$ ,  $-60.95$ , and  $-59.91\text{ }^\circ\text{C}$ , respectively. The increase in the proportion of hard segments in the molecular chain leads to the enhancement in  $T_g$ , indicating that the rigid phosphorus-containing and IPDI-derived groups limit the movement of molecular segments to a certain extent.

In Fig. 3b and c, it is demonstrated that PIDB exhibits high tensile strength and toughness, and PIDB-1 displays the best mechanical properties among all samples. In detail, the tensile strength, elongation at break, and toughness of PIDB-1 reach  $54.9\text{ MPa}$ ,  $891\%$ , and  $207.8\text{ kJ/m}^3$ , respectively, which are all much higher than those of PID (see Fig. S4 and Table S1). It indicates that the introduction of boric acid as a curing agent significantly enhances the mechanical performances of PIDB. In addition,  $0.5\text{ g}$  of rectangular PIDB-1 sample (size:  $100\text{ mm} \times 7\text{ mm} \times 0.7\text{ mm}$ ) can lift a  $10\text{ kg}$  item without breaking (see Fig. S5), further indicating its great mechanical properties. As the contents of IPDI and DOPO- $NH_2$  components increase, the rigidity of PIDB-2 and PIDB-3 gradually increases and the elasticity decreases, bringing about the reduced mechanical strength and toughness.

The cyclic tensile test was conducted on PIDB-1 sample to study its fatigue resistance. The stress-strain curves of PIDB-1 under different strains ( $50\%$ – $500\%$ ) are shown in Fig. 3d, and those under  $100\%$  strain for different cycles are displayed in Fig. 3e. In Fig. 3d, the hysteresis loop and dissipated energy increase gradually with the increase of tensile strain. Under  $100\%$  strain, the hysteresis area obviously reduces as the tensile cycle increases (see Fig. 3e). When delaying the recovery time to  $1\text{ h}$ , the stress-strain curve is close to that of the first cycle, indicative of the time-dependent self-recovery ability of PIDB-1 [39]. During stretching, abundant H bonds within the network of PIDB-1 are broken and reformed, leading to dissipation of energy, thus achieving great mechanical properties [40,41].

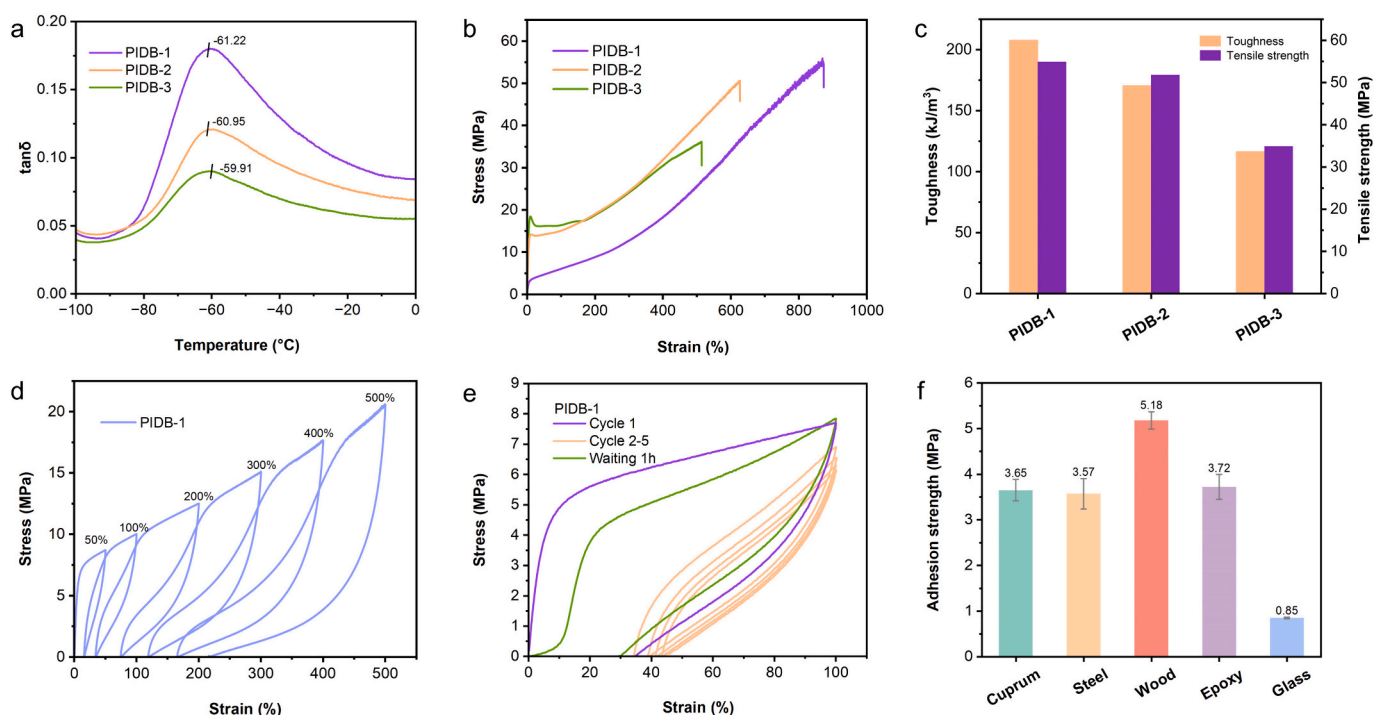


**Fig. 3.** (a)  $\tan \delta$  and (b) tensile stress-strain curves of PIDB-1, PIDB-2, and PIDB-3, (c) toughness and tensile strength of PIDB-1, PIDB-2, and PIDB-3, (d) cyclic tensile stress-strain plots of PIDB-1 under different strains, (e) cyclic tensile stress-strain plots of PIDB-1 under  $100\%$  strain, and (f) adhesion strengths of PIDB-1 on different substrates.

Polyurethane is widely used as coating and adhesive in various industries due to its excellent adhesive properties [42–44]. Hence, we conducted single lap shear tests of PIDB-1 on cuprum, steel, wood, epoxy resin (EP), and glass substrates, respectively. The lap specimens were prepared by fixing the PIDB-1 mixture between the substrates and curing it at 80 °C for 4 h (see Fig. S6 and S7). As presented in Fig. 3f and S3 and Table S2, the bonding strengths of PIDB-1 to cuprum, steel, wood, EP, and glass are 3.6, 3.5, 5.2, 3.7, and 0.8 MPa, respectively. The results demonstrate that PIDB-1 exhibits great mechanical and adhesive properties because its network contains a great deal of H-bonding interactions, making it suitable for various applications.

### 3.3. Thermal stability and fire safety of PIDB samples

The thermogravimetric (TG) and derivative TG (DTG) plots of PIDB samples are presented in Fig. 4a and b, with characteristic thermal parameters summarized in Table 2, including the temperature at 5 % mass loss ( $T_{5\%}$ ), the temperature at the maximum mass loss rate ( $T_{max}$ ), and the char yield at 800 °C (CY). All PIDB samples exhibit similar thermal degradation behaviors under nitrogen atmosphere. The  $T_{5\%}$  values for PIDB-1, PIDB-2, and PIDB-3 are 304, 305, and 290 °C, and their  $T_{max}$  values are 398, 389, and 392 °C. Notably, the char yield of PIDB-3 reaches 6.3 %, which is 44 % higher than that of PIDB-1 (2.8 %), demonstrating that the P-containing groups promote the carbonization of the matrix at high temperatures.

The flame retardancy of PIDB samples was initially assessed through the UL-94 test, with results summarized in Table 2. All PIDB elastomers achieve the UL-94 V-0 rating, demonstrating its self-extinguishing and anti-dripping ability. Without boric acid, the PID sample can only achieve a UL-94 V-2 rating, which demonstrates the positive effect of boric acid on suppressing the generation of molten droplets during combustion. Additionally, the self-extinguishing performances of PIDB

elastomers were further evaluated by igniting them (film size: 10 mm × 10 mm × 0.5 mm) on an alcohol blowtorch. As depicted in Fig. 4c, all PIDB can self-extinguish within 3 s, which is consistent with the UL-94 results. Thus, the PIDB elastomers feature satisfied flame retardancy.

The flame-retardant properties of PIDB elastomers were also assessed by using micro-cone calorimetry (MCC). As shown in Fig. S8 and Table 2, the peak heat release rate (pHRR) values of all PIDB samples are about 613–744 W/g, and those of PIDB-2 and PIDB-3 are obviously lower than that of PIDB-1, indicative of the positive effect of P-containing groups on the flame retardancy. Similar phenomenon can also be found in the total heat release (THR, see Table 2). In conclusion, the incorporation of P-based flame retardants significantly enhances the fire resistance of PIDB, which is conducive to expanding its applications.

### 3.4. Physical and chemical recyclability

As depicted in Fig. 5a, PIDB-1, PIDB-2, and PIDB-3 exhibit a transition from the glassy state to the rubbery state as temperature increases, indicating the molecular chain changes from a frozen state to a thawed state. The storage modulus of PIDB at room temperature is increased with increasing IPDI and DOPO-NH<sub>2</sub> contents, further indicating that their introduction increases the rigidity of PIDB.

Due to the existence of dynamic borate ester bonds, PIDB-1 can rearrange its network topology when it is heated above the topological freezing transition temperature ( $T_v$ ), thereby realizing recycling [27,45]. Consequently, the network topology rearrangement of PIDB-1 was studied by stress relaxation testing. According to Maxwell model, the relaxation time ( $\tau$ ) of a polymer is typically defined as the time required for its modulus ( $G$ ) to decrease to 1/e of the original modulus ( $G_0$ ). Fig. 5b shows the stress relaxation curves of PIDB-1 at 110, 120, 130, and 140 °C, respectively. Clearly, the relaxation time decreases with increasing temperature from 508 s (at 120 °C) to 45 s (at 140 °C).

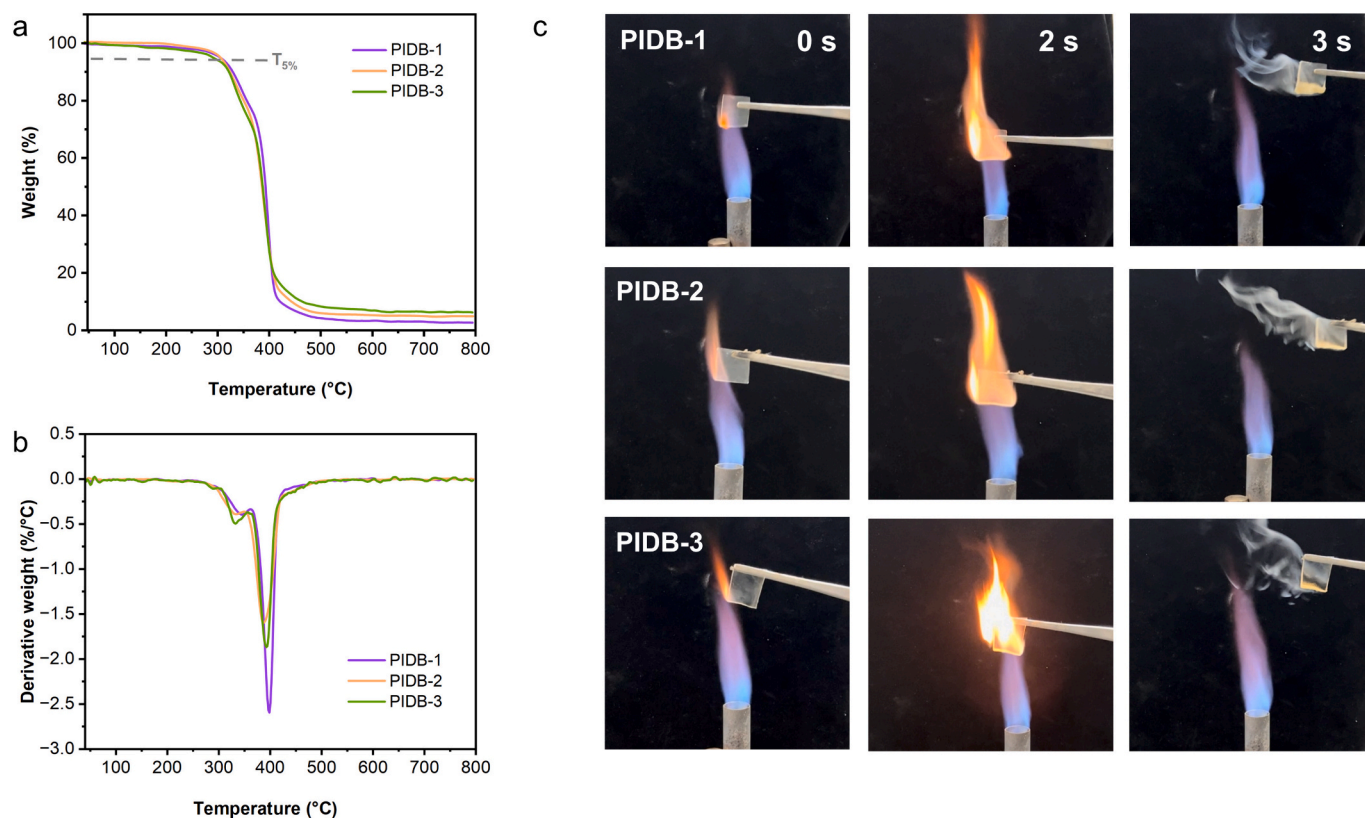
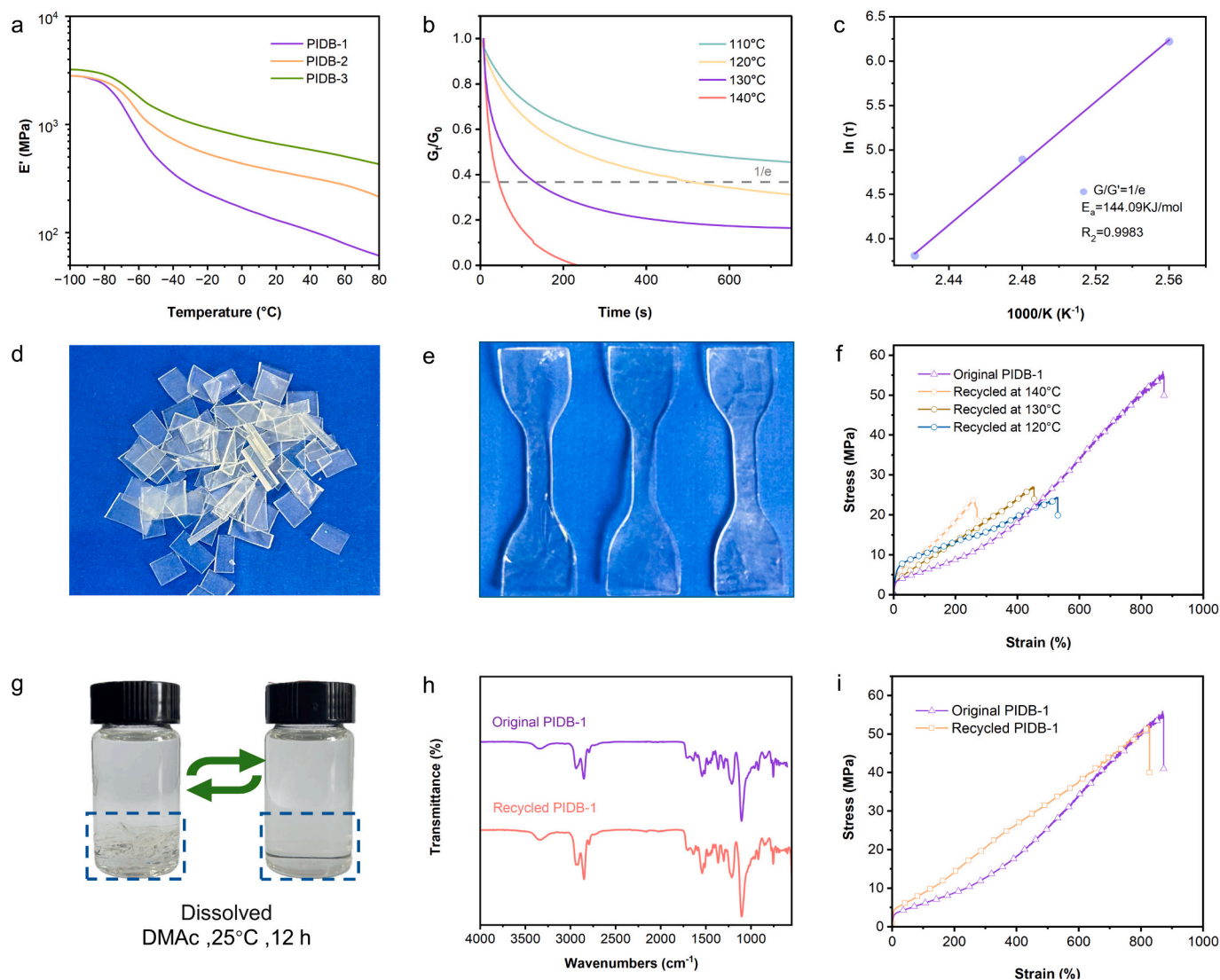


Fig. 4. (a) TG and (b) DTG curved of PIDB samples in N<sub>2</sub> conditions, and (c) digital images of PIDB samples on an alcohol blowtorch.

**Table 2**  
The thermal and combustion parameters of PIDB samples.

| Sample | $T_g$<br>(°C) | $T_{5\%}$<br>(°C) | $T_{max}$<br>(°C) | CY<br>(%) | UL-94 (3 mm) |        | pHRR<br>(W/g) | THR<br>(kJ/g) |
|--------|---------------|-------------------|-------------------|-----------|--------------|--------|---------------|---------------|
|        |               |                   |                   |           | Dripping     | Rating |               |               |
| PIDB-1 | -61           | 304               | 398               | 2.8       | No           | V-0    | 744.3 ± 21.2  | 28.5 ± 1.5    |
| PIDB-2 | -60           | 305               | 389               | 4.9       | No           | V-0    | 613.8 ± 42.5  | 27.4 ± 2.0    |
| PIDB-3 | -59           | 290               | 392               | 6.3       | No           | V-0    | 633.5 ± 15.5  | 27.8 ± 1.2    |



**Fig. 5.** (a) Storage modulus and (b) stress relaxation curves of PIDB-1, (c) the linear fitting curve of PIDB-1 based on the Arrhenius equation, the digital images of (d) broken PIDB-1 fragments and (e) reformed PIDB-1 specimens after hot-pressing, (f) tensile stress-strain curves of the reformed PIDB-1 specimens after hot-pressing at different temperatures, (g) the digital image of PIDB-1 fragments dissolved in DMAC, (h) FTIR spectra of original and chemically-recycled PIDB-1, and (i) tensile stress-strain curves of original and chemically-recycled PIDB-1.

This is probably because the mobility of chain segments and the exchange rate of dynamic borate ester bonds accelerate with increasing temperature, leading to the reduced relaxation time.

According to Fig. 5c, it is evident that the relationship between temperature and the relaxation time of PIDB-1 follows the Arrhenius equation from 120 to 140 °C.

$$\ln \tau = \frac{E_a}{RT} - \ln A$$

where  $A$  is the preexponential factor,  $R$  is  $8.314 \text{ J mol}^{-1} \text{ K}^{-1}$ , and  $E_a$  is the activation energy of the dynamic transesterification reaction.

Through linear fitting ( $R^2 = 0.9983$ ), the activation energy ( $E_a$ ) of the dynamic borate ester exchange reaction within the PIDB-1 network is determined to be  $144.09 \text{ kJ/mol}$ , which is in the range of  $E_a$  for borate ester exchange reaction reported in previous works [45,46]. To investigate the physical recycling and reprocessing capabilities of PIDB-1, it was segmented and the broken fragments were hot pressed at different temperatures for 15 min under 8 MPa to reform the transparent films (see Fig. 5d and e) [47]. The tensile properties of the reformed films were investigated, with the stress-strain curves shown in Fig. 5f. It is evident that after hot-pressing, the regenerated PIDB-1 films show reduced tensile strength, but it can still reach 46 % of the original strength.

In addition to physical recovery, PIDB-1 can also be chemically recycled by dissolving it in DMAc at room temperature (see Fig. 5g). To confirm the chemical structure of the film before and after dissolution, the FTIR tests were conducted on the original and chemically-recycled PIDB-1 films [48]. As depicted in Fig. 5h, the FTIR spectra of the original and chemically-recycled PIDB-1 films are basically the same, indicating that the chemical structure does not change after chemical recycling. Moreover, the tensile strength of the recycled film reaches 93 % of the original strength. All these results indicate that PIDB-1 can be chemically recycled in mild conditions.

### 3.5. Recycling of carbon fiber from carbon fiber-reinforced PIDB-1 composite

Carbon fiber-reinforced polymer (CFRP) composites possess outstanding mechanical properties and chemical resistance, enable them to find ubiquitous applications in various industries [49]. Carbon fiber is expensive, but its recycling is difficult since the non-degradability of the thermosetting resin as the polymer matrix. The development of degradable polymer matrices for CFRP is considered a promising solution to this dilemma [50]. Thus, the CF-reinforced PIDB-1 composites (mass ratio of CF to PIDB-1 = 60:40) were prepared using a

manual impregnation method [51]. The obtained CF-reinforced PIDB-1 composite was soaked in DMAc at room temperature for 24 h, and then the recycled CFs were washed with deionized water for several times. The microstructure of the recycled CFs was investigated by SEM, with the images shown in Fig. 6a-f. Obviously, the microstructure of the recycled CFs is very close to that of the original CFs, indicating that the CFs can be easily recycled from the CF-reinforced PIDB-1 composite. To quantitatively evaluate the performances of the recycled CFs, the tensile test and Raman analysis were conducted on them, with the results presented in Fig. 6g-i. As shown in Fig. 6g, the tensile strength of the recycled CF is only reduced by 0.6 % compared with that of the original CF, further indicating that the CF of the CF-reinforced PIDB-1 composite can be recycled. Fig. 6h and i show the Raman spectra of the original and recycled CF, respectively. The D peak at  $1360\text{ cm}^{-1}$  belongs to the disordered carbon structure, and the G peak at  $1605\text{ cm}^{-1}$  belongs to the graphitized carbon structure. The integrated area ratio of D peak to G peak ( $I_D/I_G$ ) signifies the degree of graphitization of the carbon material. Notably, the  $I_D/I_G$  of the recycled CF is basically the same with that of the original CF. All these results confirm that using PIDB-1 as a polymer matrix is an effective method for the fabrication of recyclable CFRP composites.

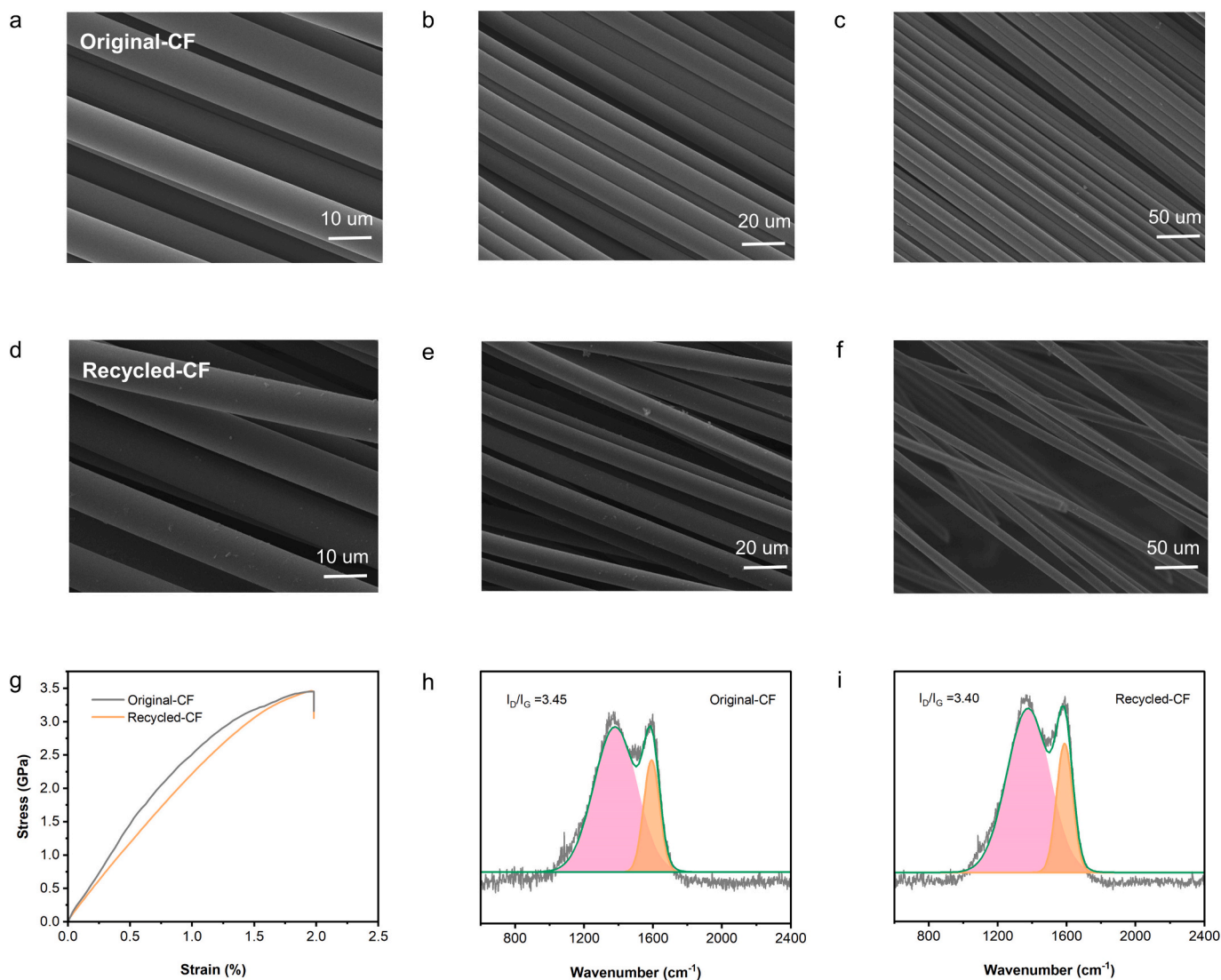


**Fig. 6.** SEM images of (a-c) original carbon fiber and (d-f) recycled carbon fiber, (g) tensile stress-strain curves of original and recycled carbon fibers, and Raman spectra of (h) original and (i) recycled carbon fibers.

#### 4. Conclusion

In this study, a flame-retardant, recyclable polyurethane elastomer with superior mechanical properties was successfully prepared based on dynamic borate esters. Due to the existence of abundant dynamic hydrogen bonds, PIDB-1 exhibits high tensile strength and toughness of 54.5 MPa and 207.8 kJ/m<sup>3</sup>, with good adhesion towards different substrates. The introduction of phosphorus and boron elements endows PIDB-1 with satisfactory flame retardancy and self-extinguishing ability, and thus it can pass an UL-94 V-0 rating. It is noteworthy that PIDB-1 features physical and chemical recyclability, and thus it can be used as an advanced polymer matrix for the fabrication of recyclable CFRP composites. Thus, this work offers an effective strategy for the development of recyclable high-performance polyurethane elastomers and carbon fiber-reinforced polymer composites.

#### CRedit authorship contribution statement

**Tiantian Zhang:** Writing – original draft, Investigation, Data curation. **Siqi Huo:** Writing – review & editing, Project administration, Conceptualization. **Guofeng Ye:** Formal analysis. **Cheng Wang:** Visualization. **Qi Zhang:** Investigation. **Zhitian Liu:** Supervision, Project administration.

#### Declaration of competing interest

The authors declare that they have no known competing financial interests or personal relationships that could have appeared to influence the work reported in this paper.

#### Data availability

Data will be made available on request.

#### Acknowledgements

This work was supported by the Australian Research Council (DE230100616), and Wuhan Institute of Technology Graduate Innovation Education Fund (CX2023100).

#### Appendix A. Supplementary data

Supplementary data to this article can be found online at <https://doi.org/10.1016/j.reactfunctpolym.2024.106056>.

#### References

- [1] J. Herzberger, J.M. Sistine, C.B. Williams, et al., Polymer design for 3D printing elastomers: recent advances in structure, properties, and printing, *Prog. Polym. Sci.* 97 (2019) 101144, <https://doi.org/10.1016/j.progpolymsci.2019.101144>.
- [2] D.K. Schneiderman, M.E. Vanderlaan, A.M. Mannion, et al., Chemically recyclable biobased polyurethanes, *ACS Macro Lett.* 5 (2016) 515–518, <https://doi.org/10.1021/acsmacrolett.6b00193>.
- [3] X. Gao, W. Fan, W. Zhu, et al., Tough and healable elastomers via dynamic integrated moiety comprising covalent and noncovalent interactions, *Chem. Mater.* 34 (2022) 2981–2988, <https://doi.org/10.1021/acs.chemmater.1c03813>.
- [4] S. Wang, X. Chen, L. Guo, et al., A human muscle-inspired, high strength, good elastic recoverability, room-temperature self-healing, and recyclable polyurethane elastomer based on dynamic bonds, *Compos. Sci. Technol.* 248 (2024) 110457, <https://doi.org/10.1016/j.compscitech.2024.110457>.
- [5] Y. Xue, M. Zhang, S. Huo, et al., Engineered functional segments enabled mechanically robust, intrinsically fire-retardant, switchable, degradable Polyurethane adhesives, *Adv. Funct. Mater.* (2024) 2409139, <https://doi.org/10.1002/adfm.202409139>.
- [6] M.M. Duran, G. Moro, Y. Zhang, et al., 3D printing of silicone and polyurethane elastomers for medical device application: a review, *Adv. Ind. Manuf. Eng.* (2023) 100125, <https://doi.org/10.1016/j.aime.2023.100125>.
- [7] B. Turner, S. Ramesh, S. Menegatti, et al., Resorbable elastomers for implantable medical devices: highlights and applications, *Polym. Int.* 71 (2022) 552–561, <https://doi.org/10.1002/pi.6349>.
- [8] Y. Yao, M. Xiao, W. Liu, A short review on self-healing thermoplastic polyurethanes, *Macromol. Chem. Phys.* 222 (2021) 202100002, <https://doi.org/10.1002/macp.202100002>.
- [9] J. Zhang, R. Hao, X. Tian, et al., Preparation and performance study of modified soybean oil polyurethane foam used for soccer equipment, *J. Appl. Polym. Sci.* 140 (2023) e54071, <https://doi.org/10.1002/app.54071>.
- [10] W.-J. Lee, H.-G. Oh, S.-H. Cha, A brief review of self-healing polyurethane based on dynamic chemistry, *Macromol. Res.* 29 (2021) 649–664, <https://doi.org/10.1007/s13233-021-9088-2>.
- [11] A. Llevot, M.A.R. Meier, Perspective: green polyurethane synthesis for coating applications, *Polym. Int.* 68 (2019) 826–831, <https://doi.org/10.1002/pi.5655>.
- [12] A. Magnin, E. Pollet, V. Phalip, et al., Evaluation of biological degradation of polyurethanes, *Biotechnol. Adv.* 39 (2020) 107457, <https://doi.org/10.1016/j.biotechadv.2019.107457>.
- [13] P.M. Paraskar, M.S. Prabhudesai, V.M. Hatkar, et al., Vegetable oil based polyurethane coatings—a sustainable approach: a review, *Prog. Org. Coat.* 156 (2021) 106267, <https://doi.org/10.1016/j.porgcoat.2021.106267>.
- [14] M.C. Damien Montarnal, François Tournilhac, Ludwik Leibler, Silica-like malleable materials from permanent organic networks, *Science* 334 (2011) 965–968, <https://doi.org/10.1126/science.1212648>.
- [15] C. Hu, J. Li, X. Pan, et al., Intrinsically flame-retardant vanillin-based PU networks with self-healing and reprocessing performances, *Ind. Crop. Prod.* 200 (2023) 116828, <https://doi.org/10.1016/j.indcrop.2023.116828>.
- [16] B. Li, G. Zhu, Y. Hao, et al., High-performance epoxy vitrimer composites based on double dynamic covalent bonds, *J. Polym. Sci.* 62 (2024) 1468–1479, <https://doi.org/10.1002/pol.20230819>.
- [17] G. Ye, C. Wang, Q. Zhang, et al., Bio-derived Schiff base vitrimer with outstanding flame retardancy, toughness, antibacterial, dielectric and recycling properties, *Int. J. Biol. Macromol.* 278 (2024) 134933, <https://doi.org/10.1016/j.ijbiomac.2024.134933>.
- [18] M. Wang, H. Gao, Z. Wang, et al., Rapid self-healed vitrimers via tailored hydroxyl esters and disulfide bonds, *Polymer* 248 (2022) 124801, <https://doi.org/10.1016/j.polymer.2022.124801>.
- [19] N. Tratnik, N.R. Tanguy, N. Yan, Recyclable, self-strengthening starch-based epoxy vitrimer facilitated by exchangeable disulfide bonds, *Chem. Eng. J.* 451 (2023) 138610, <https://doi.org/10.1016/j.cej.2022.138610>.
- [20] C. Wang, H. Xu, Z. Xie, et al., Extrudable, robust and recyclable bio-based epoxy vitrimer via tailoring the topology of a dual dynamic-covalent-bond network, *Polymer* 289 (2023) 126487, <https://doi.org/10.1016/j.polymer.2023.126487>.
- [21] L. Zhu, L. Xu, S. Jie, et al., Preparation of styrene-butadiene rubber vitrimers with high strength and toughness through imine and hydrogen bonds, *Ind. Eng. Chem. Res.* 62 (2022) 2299–2308, <https://doi.org/10.1021/acs.iecr.2c03133>.
- [22] G. Li, P. Zhang, S. Huo, et al., Mechanically strong, thermally healable, and recyclable epoxy vitrimers enabled by ZnAl-layer double hydroxides, *ACS Sustain. Chem. Eng.* 9 (2021) 13595–13605, <https://doi.org/10.1021/acscuschemeng.0c08636>.
- [23] G. Ye, S. Huo, C. Wang, et al., Strong yet tough catalyst-free transesterification vitrimer with excellent fire-retardancy, durability, and closed-loop recyclability, *Small* (2024) 2404634, <https://doi.org/10.1002/smll.202404634>.
- [24] L.L. Robinson, J.L. Self, A.D. Fusi, et al., Chemical and mechanical Tunability of 3D-printed dynamic covalent networks based on Boronate esters, *ACS Macro Lett.* 10 (2021) 857–863, <https://doi.org/10.1021/acsmacrolett.1c00257>.
- [25] C. Bao, X. Zhang, P. Yu, et al., Facile fabrication of degradable polyurethane thermosets with high mechanical strength and toughness via the cross-linking of triple boron-urethane bonds, *J. Mater. Chem. A* 9 (2021) 22410–22417, <https://doi.org/10.1039/d1ta06314f>.
- [26] X. Huang, Y. Chen, X. Lin, et al., A reusable soy protein adhesive with enhanced weather resistance through construction of a cutin-like structure, *Cell Rep. Phys. Sci.* 5 (2024) 102024, <https://doi.org/10.1016/j.xcrp.2024.102024>.
- [27] C. Li, Y. Chen, Y. Zeng, et al., Strong and recyclable soybean oil-based epoxy adhesives based on dynamic borate, *Eur. Polym. J.* 162 (2022) 110923, <https://doi.org/10.1016/j.eurpolymj.2021.110923>.
- [28] S. Yang, S. Wang, X. Du, et al., Mechanically robust self-healing and recyclable flame-retarded polyurethane elastomer based on thermoreversible crosslinking network and multiple hydrogen bonds, *Chem. Eng. J.* 391 (2020) 123544, <https://doi.org/10.1016/j.cej.2019.123544>.
- [29] H. Wang, Y. Fu, Y. Liu, et al., Synthesis of facilely healable and recyclable imine vitrimers using biobased branched diamine and vanillin, *Eur. Polym. J.* 196 (2023) 112309, <https://doi.org/10.1016/j.eurpolymj.2023.112309>.
- [30] Y. Xue, J. Lin, T. Wan, et al., Stretchable, ultratough, and intrinsically self-extinguishing elastomers with desirable recyclability, *Adv. Sci.* 10 (2023) 2207268, <https://doi.org/10.1002/advs.202207268>.
- [31] S. Wang, S. Lou, P. Fan, et al., A novel aromatic imine-containing DOPO-based reactive flame retardant towards enhanced flame-retardant and mechanical properties of epoxy resin, *Polym. Degrad. Stab.* 213 (2023) 110364, <https://doi.org/10.1016/j.polymdegradstab.2023.110364>.
- [32] C. Wang, S. Huo, G. Ye, et al., A P/Si-containing polyethylenimine curing agent towards transparent, durable fire-safe, mechanically-robust and tough epoxy resins, *Chem. Eng. J.* 451 (2023) 138768, <https://doi.org/10.1016/j.cej.2022.138768>.
- [33] X. Ma, X. Wang, H. Zhao, et al., High-performance, light-stimulation healable, and closed-loop recyclable lignin-based covalent adaptable networks, *Small* 19 (2023) 2303215, <https://doi.org/10.1002/smll.202303215>.
- [34] C. Tong, S. Zhang, T. Zhong, et al., Highly fibrillated and intrinsically flame-retardant nanofibrillated cellulose for transparent mineral filler-free fire-protective

- coatings, *Chem. Eng. J.* 419 (2021) 129440, <https://doi.org/10.1016/j.cej.2021.129440>.
- [35] X. Shang, Y. Jin, W. Du, et al., Flame-retardant and self-healing waterborne polyurethane based on organic selenium, *ACS Appl. Mater. Interfaces* 15 (2023) 16118–16131, <https://doi.org/10.1021/acsami.3c02251>.
- [36] D.-M. Xie, Y.-X. Zhang, Y.-D. Li, et al., Castor oil-derived sustainable poly(urethane urea) covalent adaptable networks with tunable mechanical properties and multiple recyclability based on reversible piperidine-urea bond, *Chem. Eng. J.* 446 (2022) 137071, <https://doi.org/10.1016/j.cej.2022.137071>.
- [37] Q. Shi, S. Huo, C. Wang, et al., A phosphorus/silicon-based, hyperbranched polymer for high-performance, fire-safe, transparent epoxy resins, *Polym. Degrad. Stab.* 203 (2022) 110065, <https://doi.org/10.1016/j.polymdegradstab.2022.110065>.
- [38] B. Zhang, X. Yang, X. Lin, et al., High-strength, self-healing, recyclable, and catalyst-free bio-based non-isocyanate polyurethane, *ACS Sustain. Chem. Eng.* 11 (2023) 6100–6113, <https://doi.org/10.1021/acsschemeng.3c01181>.
- [39] Y. Song, J. Li, G. Song, et al., Tough and self-healing waterborne polyurethane elastomers via dynamic hydrogen bonds design for flexible conductive substrate applications, *ACS Appl. Mater. Interfaces* 16 (2024) 2683–2691, <https://doi.org/10.1021/acsami.3c12688>.
- [40] Z. Zhang, L. Qian, G. Huang, et al., Insertion of urea moieties for one-component strong yet tough, self-healing polyurea protective materials, *Adv. Funct. Mater.* 34 (2023) 2310603, <https://doi.org/10.1002/adfm.202310603>.
- [41] L. Lu, J. Xu, J. Li, et al., High-toughness and intrinsically self-healing cross-linked polyurea elastomers with dynamic sextuple H-bonds, *Macromolecules* 57 (2024) 2100–2109, <https://doi.org/10.1021/acs.macromol.3c02202>.
- [42] F. Van Lijsebetten, T. Maiheu, J.M. Winne, et al., Epoxy adhesives with reversible hardeners: controllable thermal debonding in bulk and at interfaces, *Adv. Mater.* 35 (2023) 2300802, <https://doi.org/10.1002/adma.202300802>.
- [43] C.R. Westerman, B.C. McGill, J.J. Wilker, Sustainably sourced components to generate high-strength adhesives, *Nature* 621 (2023) 306–311, <https://doi.org/10.1038/s41586-023-06335-7>.
- [44] B. Zheng, T. Liu, J. Liu, et al., Spider silk-inspired dynamic covalent polyurethane with fast repairing, shape memory, and strong dynamic adhesion via lignin enhanced microphase separation, *Compos. Part B* 257 (2023) 110697, <https://doi.org/10.1016/j.compositesb.2023.110697>.
- [45] Z. Guo, C. Bao, X. Wang, et al., Room-temperature healable, recyclable and mechanically super-strong poly(urea-urethane)s cross-linked with nitrogen-coordinated boroxines, *J. Mater. Chem. A* 9 (2021) 11025–11032, <https://doi.org/10.1039/d1ta00902h>.
- [46] Z.H. Zhao, C.H. Li, J.L. Zuo, Dynamic polymeric materials based on reversible B–O bonds with dative boron–nitrogen coordination, *SmartMat* 4 (2023), <https://doi.org/10.1002/smm2.1187>.
- [47] W. Yang, Q. Yi, F. Liu, et al., Fabrication of malleable, repairable, weldable, recyclable and robust epoxy vitrimers from itaconic acid for recycled adhesion, *Eur. Polym. J.* 196 (2023) 112278, <https://doi.org/10.1016/j.eurpolymj.2023.112278>.
- [48] C. Bao, R. Miao, Y. Yin, et al., Mechanically robust yet body-temperature self-healable polyurethane elastomer via the cross-linking of dynamic boroxines, *ACS Appl. Polym. Mater.* 6 (2023) 797–805, <https://doi.org/10.1021/acsapm.3c02418>.
- [49] T. Yang, X. Lu, X. Wang, et al., Upcycling of carbon fiber/thermoset composites into high-performance elastomers and repurposed carbon fibers, *Angew. Chem. Int. Ed.* 63 (2024) 202403972, <https://doi.org/10.1002/anie.202403972>.
- [50] C. Tretbar, J. Castro, K. Yokoyama, et al., Fluoride-catalyzed siloxane exchange as a robust dynamic chemistry for high-performance vitrimers, *Adv. Mater.* 35 (2023) 2303280, <https://doi.org/10.1002/adma.202303280>.
- [51] C. Huyan, D. Liu, C. Pan, et al., Thermally recyclable and reprocessable glass fiber reinforced high performance thermosetting polyurethane vitrimer composites, *Chem. Eng. J.* 471 (2023) 144478, <https://doi.org/10.1016/j.cej.2023.144478>.